14th European Signal Processing Conference (EUSIPCO 2006), Florence, Italy, September 4-8, 2006, copyright by EURASIP

DETECTION PERFORMANCE FOR THE GMF APPLIED TO STAP DATA

Sébastien MARIA, Jean-Jacques Fuchs

IRISA/Université de Rennes I
Campus de Beaulieu - 35042 Rennes Cedex - France
phone: + (33) 299 84 71 62, fax: + (33) 299 84 71 71, email: sebastien.maria@irisa.fr

ABSTRACT

A major problem with most standard methods working on STAP data is their lack of robustness in the presence of heterogeneous clutter background. Indeed most of them rely on the assumption that the clutter remains homogeneous over quite a large range. We apply to the STAP data, a high-resolution method called the Global Matched Filter (GMF). Since it models and identifies both the interferences (clutter and jammer(s)) and the target(s) from the data by only using the snapshot of interest, it solves the above mentioned difficulty. We describe here how to apply the GMF to the STAP data and we compare its performance to the other STAP methods by establishing the target detection probability for a constant false alarm rate.

1. INTRODUCTION

Radar technology has vastly evolved over the last 50 years but most progress has been made in the past two decades. A requirement of next generation airborne radar is to detect targets in a perturbation background comprising interferences (clutter and potentially jammer) and noise. In this aim space-time adaptive processing (STAP) has been proposed as a leading technology for improving the performance of detection algorithms [1, 2].

As clutter suppression is critical to surveillance radar, the need for adaptive methods arises in practice when the statistics of the perturbation (interference plus noise) are unknown and must be inferred from the data. In moving radar platforms, the clutter may vary significantly from cell to cell, hence STAP performance is limited by how well the estimated interference plus noise covariance matrix represents the actual cell perturbation. This problem is even more important in a notably heterogeneous clutter environment.

The new approach we propose here allows to handle this type of environment. It is based on a high-resolution method denominated Global Matched Filter (GMF) [3]. This method has been developed in a sparse representation context and has many areas of application, notably in joint detection and estimation. The advantage of the GMF is its ability to separate target from clutter by relying only on the information contained in the range bin of interest. It follows that perturbation covariance matrix estimation is no longer necessary.

In this paper, we apply the GMF to STAP data and compare its performance to those of fully adaptive and partially adaptive processings by comparing the probabilities of detection (P_d) of these methods.

In Section 2, we will describe the STAP model. In Section 3 we show how to adapt the GMF method to the STAP context. Then in Section 4, we give the formulas of the probability of false alarm and detection for the currently used methods and for the GMF. Finally, we will present some simulation results in Section 5 before to conclude in Section 6.

2. PRELIMINARIES TO THE STAP

Conventional radars are able to detect targets in the time domain (range) and the frequency domain (Doppler frequency). To improve radar performance, advanced signal processing techniques have been developed. Space-time adaptive processing provides an additional dimension (space) for the detection of moving targets. The idea is to apply a two-dimensional filter (which uses both temporal and spatial filtering) in order to maximize the output signal-to-interference-plus-noise ratio ($SINR_{out}$).

For simplicity the airborne pulse-Doppler radar considered here is a multichannel receiver linear antenna array. The array consists of N_s sensors and the radar transmits a coherent burst of N_p pulses at constant pulse repetition frequency $f_r = 1/T_r$ where T_r is the pulse repetition interval (PRI). In each PRI, N_d range samples are collected. The time interval over which the waveform returns are collected is commonly referred to as the coherent-processing interval (CPI) and the data are collected in the well-known $(N_s \times N_p \times N_d)$-dimensional data cube. The data is then processed at one range of interest corresponding to a slice of the CPI data cube. This slice is converted into a $N_s N_p$-dimensional vector called snapshot. We assume that a target remains in one range gate during a CPI. If a target is present in the range gate of interest, then the snapshot 's' has contributions due to the target and the perturbations (clutter, receiver thermal noise and potentially jammer):

$$s = \alpha s_t(\tilde{\phi}; \tilde{f}) + s_{pert} \qquad (1)$$

where $\alpha; \tilde{\phi}; \tilde{f}$ are the target amplitude, normalized angle and normalized Doppler frequency respectively. Here $s_t(\tilde{\phi}; \tilde{f})$ represents the spatio-temporal steering vector associated with the target:

$$s_t(\tilde{\phi}; \tilde{f}) = u(\tilde{f}) \otimes v(\tilde{\phi})$$

where $\otimes$ represents the Kronecker tensor product and

$$u(\tilde{f}) = \begin{bmatrix} 1 & e^{-j2\pi\tilde{f}} & \cdots & e^{-j2\pi(N_p-1)\tilde{f}} \end{bmatrix}^T$$
$$v(\tilde{\phi}) = \begin{bmatrix} 1 & e^{-j2\pi\tilde{\phi}} & \cdots & e^{-j2\pi(N_s-1)\tilde{\phi}} \end{bmatrix}^T$$

are the N_p-dimensional spatial steering vector and N_s-dimensional temporal steering vector. The perturbation component s_{pert} is modeled as:

$$s_{pert} = s_c + s_j + n$$

where n represents the receiver thermal noise, s_j the contribution of the jammers and s_c the contribution of the clutter. The noise is assumed to be a zero-mean complex Gaussian random process $n \sim \mathcal{N}(0; \sigma^2 I)$. The jammer signal is

$$s_j = \sum_k \alpha_k^j \, s_t(\tilde{\phi}_j; \tilde{f}_k) \qquad (2)$$

where $\tilde{\phi}_j$ is the jammer azimuth angle, and α_k^j represents the amplitude of the received jammer signal for Doppler frequency $\tilde{f}_k$. We assume that the jammer is localized in space (i.e., has a fixed direction) but is spread in Doppler. If multiple jammers are present, a sum of terms like (2) is expected to contribute to the perturbation vector s_{pert}. The clutter component can be modeled as the sum of many targets with a complex amplitude α_k^c.

$$s_c = \sum_k \alpha_k^c \, s_t(\tilde{\phi}_k; \tilde{f}_k)$$

The main feature distinguishing clutter from moving targets is their zero speed which induces the following relation between the clutter normalized Doppler frequency and the normalized angle:

$$\tilde{f}_k = \frac{2v_{airborne}T_r}{d} \tilde{\phi}_k = \beta\tilde{\phi}_k$$

Below, we consider that the parameter β is adjusted to be equal to 1.

The space-time processor linearly combines the elements of the snapshot s yielding the scalar output

$$y = w^H s$$

where the superscript 'H' denotes conjugate transposition and w is a N_sN_p weight vector. It is well known that the weight vector maximizing the output SINR [4] is

$$w = R_{pert}^{-1} s_t(\tilde{\phi};\tilde{f}) \quad (3)$$

where $R_{pert} = E(s_{pert}s_{pert}^H)$ is the perturbation covariance matrix. To apply this processor, R_{pert} is in general estimated on the adjacent range gates of the snapshot of interest. Yet, the use of this fully adaptive STAP is infeasible in most radar applications due to both the computational cost and the large number of adjacent data vectors required (the assumption of stationary and homogeneous clutter is realistic only over a limited range around the current slice). Hence many partially adaptive (or sub-optimal) methods have been developed.

3. GLOBAL MATCHED FILTER

3.1 Description of the method

The Global Matched Filter applies to any situation where a noisy real observation vector can be modeled as a sum of noise and a small unknown number of elementary signals of a parameterized family, i.e., when the m-dimensional observation vector can be represented as

$$b = \sum_{i=1}^{p} a(\theta_i)x_i + e \quad (4)$$

where e is the additive noise vector and p is the unknown number of components to be estimated together with the θ_i's, the value of the scalar or vector of parameters and the x_i's the associated weights.

If e is assumed to be Gaussian, the maximum likelihood estimates of $(x_i;\theta_i)$ are obtained by solving the non-linear least-squares problem

$$\min_{\theta_i;\, x_i} \|b - \sum_{1}^{p} a(\theta_i)x_i\|_2^2.$$

As this problem is non linear and p is unknown, it is difficult to solve. The GMF proposes to turn it into a convex program having a large number of unknowns as follows. One uniformly discretizes the θ parameter in its domain of interest and constructs with the n columns $a_j = a(\theta_j)$ -with θ_j on a regular grid- a matrix A having thus far more columns than rows ($n \gg m$). The idea is then to seek a sparse representation of b

$$b \simeq Ax$$

where x is a parsimonious weight vector having of the order of p non zero components. One way to obtain such a parsimonious representation is to use the ℓ_1-norm. The corresponding optimization problem is thus

$$\min_x \|x\|_1; \text{ subject to } \|b - Ax\|_2^2 \le B \quad (5)$$

which is equivalent to the easy-to-solve quadratic criterion

$$\min_x \frac{1}{2}\|b - Ax\|_2^2 + h\|x\|_1; \quad h > 0 \quad (6)$$

for an adequately chosen parameter h. Note that the ℓ_1-norm penalty term ensures the sparsity of the solution whereas the ℓ_2-norm ensures the good approximation of b and h monitors the weight between both terms.

3.2 Adaptation to the STAP context

In this part we will explain how to apply the GMF to the observation model (1). Due to the particular structure of clutter and jammer, equation (1) appears to be of the same form as (4) if one identifies $(\tilde{\phi}_i;\tilde{f}_i)$ with the parameter θ_i. The only difference is that model (1) is a complex equation whereas (4) is real. Two steps are thus required to apply the GMF: transformation of the snapshot into a real vector and construction of the A matrix.

For the first step, we apply to the complex s-vector a set of standard beamformers tuned to m equispaced spatio-temporal points. This transforms the N_sN_p-dimensional complex vector s into a m-dimensional real vector that will be the input-data to the GMF, the b-vector in (6). A steering vector $s_t(\tilde{\phi}_i;\tilde{f}_i)$ is associated with each such spatial and temporal point and the corresponding beamformer-output applied to the snapshot s is:

$$b_i = |s_t(\tilde{\phi}_i;\tilde{f}_i)^H s|^2 / (N_sN_p)^2; \text{ for } i = 1..m$$

In order to keep all the information, it is suggested in [3] to take m equal to the number of degrees of freedom (d.o.f) of the covariance matrix of the snapshot. In our case, this gives $m = 2N_sN_p - 1$ which is also the number of real d.o.f. in s.

To construct the A matrix, normalized angle and Doppler frequency must be more finely discretized in their domain of definition at $n \gg m$ values $(\tilde{\phi}_j;\tilde{f}_j)$. The n corresponding steering vectors $s_t(\tilde{\phi}_j;\tilde{f}_j)$ are in turn transformed by the set of m beamformers described above. The corresponding output-vectors are normalized to one in Euclidean norm and each of them will represent a column of the $m \times n$ real matrix A. The number n is chosen large enough to allow the approach to attain the Cramer Rao bounds. In practice, for standard values of Signal-to-Noise-Ratios (SNR's), one expects to improve the standard beamformer resolution by a factor 2 or 3. Hence we propose to discretize the frequency and azimuth domain at at least $9N_p$ and $9N_s$ points. The typical dimension of A is thus $(2N_sN_p - 1) \times (81N_sN_p)$.

Since clutter and jammers can be represented by a sum of nuisance targets (zero-speed for the clutter and fixed azimuth for the jammer), one can expect that they will be estimated and detected just as the target of interest by the GMF. We will represent the output of the GMF in the way presented in Figure 2 (see Section 5) where clutter, jammer and a target are present. It consists in ploting the values of the solution x on a regular grid (see Figure 1) where each cell is associated with a couple $(\tilde{\phi}_p;\tilde{f}_q)$ that corresponds to a given column of A. Typically, one expects that clutter will be represented on the diagonal line $\tilde{\phi} = \tilde{f}$.

4. PROBABILITY OF DETECTION

4.1 Fully and partially adaptive methods

Processing STAP data consists in deciding between two hypotheses for each range bin

$$\begin{aligned} H_0: \; s &= s_{pert} \\ H_1: \; s &= \alpha s_t(\tilde{\phi};\tilde{f}) + s_{pert}. \end{aligned}$$

where $\alpha = |\alpha|e^{j\delta}$ is a complex gain whose random phase δ is uniformly distributed between 0 and 2π. Under H_0 the signal consists of interference (clutter and potentially jammer) plus noise whereas under H_1, a target signal also appears. A statistical test can be built to determine if a target is effectively present in the range bin of interest. When perturbations are assumed to be Gaussian, the random vector s, conditioned on δ, is also Gaussian. When the perturbation covariance matrix is perfectly known, the adaptive constant false alarm rate (CFAR) detection test amounts to compare the maximum, over N_sN_p couples, of the output power of the STAP filter divided by the output perturbation power to a threshold T [5, 6, 7]:

$$\max_{m;n} \left\{ \frac{\mathrm{j} s_t^H(\tilde{\phi}_m;\tilde{f}_n) R_{pert}^{-1} s \mathrm{j}^2}{s_t^H(\tilde{\phi}_m;\tilde{f}_n) R_{pert}^{-1} s_t(\tilde{\phi}_m;\tilde{f}_n)} \right\} \underset{H_0}{\overset{H_1}{?}} T \qquad (7)$$

where $s_t(\tilde{\phi}_m;\tilde{f}_n)$ are spatio-temporal steering vectors evaluated at N_s equispaced spatial points and N_p equispaced temporal points. The threshold T is fixed to achieve a given probability of false alarm (P_{fa}) as [5]

$$T = \Gamma\, ln(1 \Gamma (1 \Gamma P_{fa})^{1=N_s N_p}):$$

Since the covariance matrix R_{pert} is unknown it is usually estimated from L adjacent range bins

$$\hat{R}_{pert} = \frac{1}{L} \sum_{k=1}^{L} s_k s_k^H$$

where s_k are snapshots belonging to the neighborhood of s. One generally takes L ' $2N_s N_p$ to get an invertible reasonably accurate estimate. The CFAR test is then performed as in (7) by replacing R_{pert} with its estimate. As we have already pointed out in Section 2, this fully adaptive filter is not achievable in practice both because of computation time and lack of homogeneity of the clutter. Ward [2, 8] has developed partially adaptive processors to reduce both computational time and training requirements (smaller L). A partially adaptive STAP is defined to be a processor which is not adaptive simultaneously in both the spatial and the temporal domain. Four different STAP structures can be defined: element-space pre-doppler, element-space post-doppler, beam-space pre-doppler and beam-space post-doppler. These sub-optimal methods use reduced vectors and consequently reduced perturbation covariance matrices to perform a CFAR test similar to (7) .

4.2 The GMF

To simplify the approach, we will consider in the sequel that only clutter contributes to the interferences. In the GMF, the CFAR test (7) is replaced by an adequate choice of the parameter h in (6). In (6), h allows to tune the parsimony of x, i.e., the larger h the more parsimonious x. Under H_0 and if the perturbation is limited to the thermal noise, it is indeed possible for a given σ^2 to attain any given false alarm (a non-identically zero optimal x in (6)) rate by tuning the value of h.

But this is quite an unrealistic case and we consider now the case where clutter is present and σ^2 unknown. In the GMF we need to first estimate σ^2 which we assume to be constant over all the snapshots in the data cube. The covariance matrix of all these snapshots s_k is then estimated as

$$\hat{R} = \frac{1}{N_d} \sum_{k=1}^{N_d} s_k s_k^H$$

and it can be decomposed as

$$\hat{R} = R_t + \hat{R}_c^{global} + \hat{\sigma}^2 I \,'\, \hat{R}_c^{global} + \hat{\sigma}^2 I:$$

where R_t represents the contribution of the few targets present in the cube, $\hat{R}_c^{global}$ is the covariance matrix of all the clutter present and $\hat{\sigma}^2 I$ is the covariance matrix of the thermal noise. One can neglect R_t in this expression. The Brennan rule [9] states that the clutter matrix rank is equal to $N_s + \beta(N_p \Gamma 1)$. As $\hat{R}$ is a $(N_p \Theta N_s)$-dimensional matrix, this means that $\hat{R}_c^{global}$ is rank deficient and an estimate $\hat{\sigma}^2$ of σ^2 is then easily deduced from the smallest eigenvalues of $\hat{R}$.

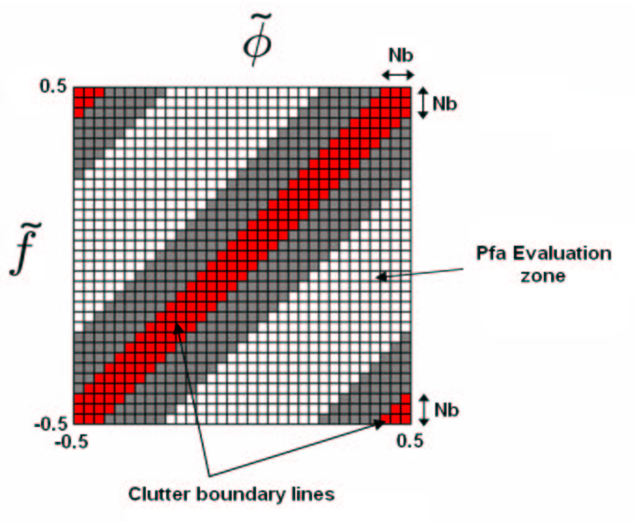

Figure 1: Representation of discretized normalized azimuth $\tilde{\phi}$ and Doppler frequency $\tilde{f}$ domain.

In contrast to fully or partially adaptive filters which seek to eliminate the clutter by *whitening* the snapshot (3), the GMF estimates it. As we have seen in Section 3.2 , the GMF will represent the clutter by targets that are on or close to the diagonal which corresponds to zero-speed targets (see Figure 2). Some spurious peaks (non zero-components in x) induced by the clutter can appear in the neighborhood of the diagonal. To achieve a given P_{fa}, we will tune h by only looking at the white zone of Figure 1 whose boundaries are fixed *a priori* and where we are sure that only the thermal noise will induce non-zero components in x. This tuning is done experimentally once and forever.

Once h is fixed in this way, one can further determine *a posteriori* the precise boundaries of the area where the clutter may induce spurious peaks (for the current h). This means that we will not be able to detect targets within this area, i.e., targets that are too slow. We thus define clutter boundary lines (see Figure 1) by introducing a parameter N_b that is experimentally fixed by performing a large number of realizations (clutter and thermal noise). Larger values of h (smaller P_{fa}) correspond to smaller N_b, finer clutter zones. For the GMF, N_b can be assimilated to the minimum detectable velocity (MDV) which is another criterion of performance [10]. In Section 5, we will comment on the tradeoff between the choice of parameter h and the MDV.

Now, for a given P_{fa}, the detection performance of the GMF for different Signal-to-Noise-Ratios can be experimentally determined. Since the probability of detection of fully and partially adaptive methods dramatically deteriorates when a target is close to the clutter ridge, we will simulate, as is usually done, targets that are far from it to compare the probability of detection of the GMF with those of the others methods. The analysis of the GMF detection performance with a target close to clutter ridge is the subject of further investigations.

5. EXPERIMENTAL RESULTS

All simulations have been performed for $N_s = N_p = 10$. The normalized azimuth and normalized Doppler frequency both belong to $[\Gamma 0{:}5; 0{:}5]$. To build b the input-vector, we discretize both spaces with a step of $0{:}07$ that leads to $m = 225$. To build the A matrix, we take a step equal to $0{:}01$ in azimuth and frequency, this gives $n = 10201$. Both values are slightly larger than the values announced in Section 3.2. essentially because we took rounded step values. As we have pointed out in Section 4.2, at each P_{fa} and noise variance σ^2 corresponds a h parameter. For instance, to have $P_{fa} = 10^{-6}$ for $\sigma^2 = 1$, we obtained experimentally that the h parameter must be fixed to $h = :30$ which in turn leads to $N_b = 15$ (to be compared to the 101 discretization steps)for reasonable value of clutter-to-noise power ratio. The two following simulations have been performed with these values.

The first simulation presents the results obtained by the GMF for a quite standard scenario with one target at $(\tilde{\phi} = \Gamma 0{:}2; \tilde{f} = 0{:}2)$ and $SNR_{out} = 20$dB. Note that the SNR_{out} is the output Signal-to-Noise-Ratio of the GMF and is thus defined as follows:

$$SNR_{out} = 10\log_{10}\left(\frac{\alpha^2 \mathrm{j} s(\tilde{\phi}_i;\tilde{f}_i)^H s_t(\tilde{\phi};\tilde{f})\mathrm{j}^2}{(N_s N_p)^2}\frac{N_s N_p}{\sigma^2}\right) \quad (8)$$
$$, \quad 10\log_{10}\left(\frac{\alpha^2}{\sigma^2}\right) + 10\log_{10}(N_s N_p)$$
$$, \quad SNR_{in} + 20\text{dB}$$

We can observe that in our configuration we have a gain of 20dB between SNR_{out} and the input Signal-to-Noise-Ratio SNR_{in}. The interferences have the following properties: the output Clutter-to-Noise-Ratio (defined in a similar way to (8)) is $CNR_{out} = 30$dB and one jammer is localized at $\tilde{\phi} = 0{:}3$ with $JNR_{out} = 30$ dB (output Jammer-to-Noise-Ratio). The GMF is applied to the corresponding (unique) snapshot and a typical representation of its output is given in Figure 2. We can see that clutter ridge and jammer are well localized whereas the target can be easily identified. Note that to solve the GMF criterion (6) with a low computational cost, efficient algorithms have been recently developed [11, 12]. With the below configuration (about ten thousand unknowns), the GMF is solved in about 3 seconds on standard desk computer.

In the second simulation we compare the detection performance of the GMF with those of the methods studied in [5]. In [5] fully and partially adaptive (reduced-dimension) methods are compared. The target to be detected is localized at $(\tilde{\phi} = 0{:}3; \tilde{f} = \Gamma 0{:}2)$. Figure 3 gives the probability of detection versus the output SNR. For fully and partially adaptive methods, detection performance principally depends on the number L of snapshots used to estimate the interference covariance matrix. The GMF performance, which only uses the snapshot of interest, has performance close to those of the partially adaptive methods when $L = 50$, i.e. five times the number of snapshots required to have an invertible estimate of the perturbation covariance matrix. Note that $L = 50$ remains too important in a transient and inhomogeneous environment and the GMF thus appears as a highly efficient alternative method to process data in such an environment.

Finally, in a last set of simulations we analyze how the detection performance varies when h increases. Increasing h amounts to diminish the P_{fa} and allows to reduce the size of the domain where the clutter may induce peaks in the output of the GMF, i.e., it allows to detect slower moving targets. We thus observe, in Figure 4, a degradation of the detection performance when h increases. Nevertheless if h is fixed to :7 for instance, the GMF detection performance is still better than those of partially adaptive methods with $L = 20$ (compare with Figure 3). Note that for $h = :7$ the clutter resolution width becomes $N_b = 7$, it was equal to 15 for $h = :30$. We have not estimated the corresponding P_{fa} which is extremely small.

6. CONCLUSION

Many efforts have been done during last decade to reduce the number of adjacent range gates required to estimate the perturbation covariance matrix and provide more robust filters in severely heterogeneous clutter environments. These improvements have been essentially performed with reduced-dimension techniques [2] or with reduced-rank techniques [13, 14, 15]. The GMF appears as a powerful method to circumvent the covariance estimation problem. Since the GMF identifies both the targets and a model of the interferences it has the advantage to be able to work on a single snapshot without prior estimation of the perturbation covariance matrix. In this preliminary study of the application of the GMF to STAP data, we compared the detection performance of the GMF to those of a representative reduced-dimension method.

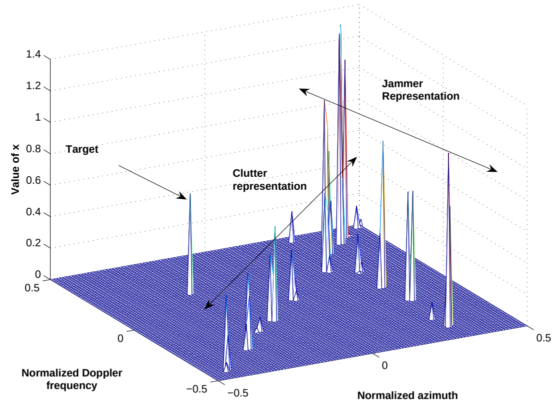

Figure 2: Typical representation of the GMF.

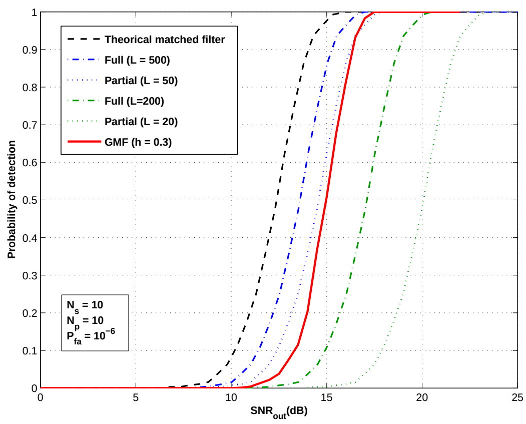

Figure 3: Probability of Detection for fully and partially adaptive STAP and the GMF.

REFERENCES

[1] Klemm R., "Principles of space-time adaptive processing". *IEE Radar, Sonar, Navigation and avionics*, series 12, 2002.

[2] Ward J., "Space-Time Adaptive Processing for Airborne Radar". *Lincoln Laboratory Technical Report 1015*, Dec. 1994.

[3] Fuchs J.J., "On the application of the global matched". filter to DOA estimation with uniform circular arrays. *IEEE Trans on S.P.*, vol. 49, p. 702–709, avr. 2001.

[4] Brennan L.E., Mallett J.D. and Reed I.S., "Adaptive Arrays in Airborne MTI Radar". *IEEE Trans. on Antennas and Propagation* vol. AP-24, 607-615, Sept. 1976.

[5] Reed I.S., Gau Y.L., and Truong T.K., "CFAR detection and estimation for STAP radar". *IEEE Trans. on A.E.S*, vol. 34, 3, july 1998.

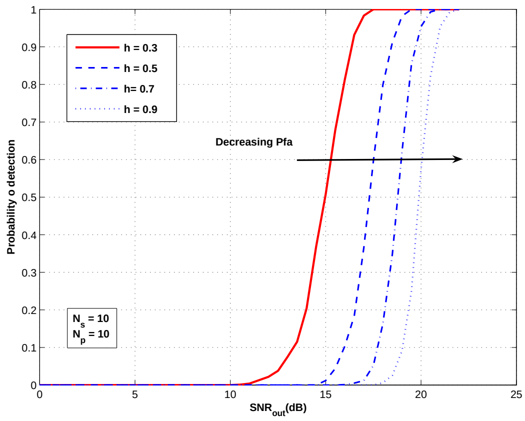

Figure 4: Evolution of detection probability for different values of h.

[6] Melvin W.L., “A STAP overview”. *IEEE A&E systems magazine*, vol. 19, 1, 19-35, Part 2: Tutorials, jan. 2004.

[7] Goldstein J.S. and Reed I.S., “Theory of partially Adaptive Radar”. *IEEE Trans. on A.E.S*, vol. 33, 4, oct. 1997.

[8] Ward J., Kogon S.M., “Space-Time Adaptive Processing (STAP) for AMTI and GMTI radar”. *Proceedings of IEEE Radar Conference*, Philadelphia Pennsylvania, 26-29 april 2004 .

[9] Brennan L.E. and Reed I.S., “Theory of adaptive radar”. *IEEE Trans. on A.E.S*, vol. 9, 237-251, 1973.

[10] Picciolo M., Nguyen N. and Andrew G.A., “An investigation of space-time adaptive processing with regard to minimum detectable velocity”. *Naval Research Laboratory Technical Report*, NRL/MR/5315-99-8383, 1-23, june 1999.

[11] Malioutov D.M., Cetin M. and Willsky A.S., “Homotopy continuation for sparse signal representation” *IEEE ICASSP*, V, 733-737, Philadelphia,, 2005.

[12] Efron B., Hastie T., Johnstone I. and Tibshirani R., “Least angle regression,” *Annals of Statistics*, vol. 32, 407–499, Apr. 2004.

[13] Goldstein J.S. and Reed I.S., “Reduced rank adaptive filtering”. *IEEE Trans. on S.P.*, vol. 45, 2, 492-496, Feb. 1997.

[14] Kirsteins I. and Tufts D., “Adaptive detection using low rank approximation to a data matrix”. *IEEE Trans. on A.E.S*, vol. 30, 1, 55-67, jan. 1994.

[15] Rangaswany M., Freeman C. L., Gerlach K.R., “Robust adaptive signal processing methods for heterogeneous radar clutter scenarios”. *Signal Processing*, vol. 84, 9, 1625-1636, sept. 2004.